1

Introduction to Additive Manufacturing

Every human-made object around us has a unique history. This history is the evolution of raw materials that are extracted from the earth through human intervention and made into a usable form. The development of humankind has always been linked to modifying the history of raw material evolution into a usable product (manufacturing) in the pursuit of making it more efficient and flexible. Today, in the early decades of the twenty-first century, additive manufacturing (AM) is the most advanced and cutting-edge technique used in manufacturing. It entered the limelight as '*3D printing*' and has flipped the tables in research and development with a paradigm shift, gradually ushering in the fourth Industrial Revolution. However, we can only recognize the full worth of AM by understanding traditional manufacturing techniques and their evolution. This chapter first presents the history of manufacturing and the AM approach. It addresses the advantage of AM over conventional manufacturing while considering the challenges AM currently faces. The remainder of the chapter introduces laser-based AM, which is at the forefront of AM techniques. Overall, understanding the fundamental aspects of these techniques and their effects is the primary goal of this book.

1.1 Evolution of Manufacturing

Manufacturing is the process of forming a usable product out of raw materials using manual labor or mechanical machinery. The archaeological evidence for manufacturing dates back to the Stone Age, when *Homo habilis* produced the earliest tools carved out of stones [De la Torre, 2011]. This record suggests a subtractive manufacturing technique, where material is removed from a single piece to transform it into another usable form. Other techniques emerged progressively, including joining, machining, casting, and transformation (deformation) of materials. However, these processes were carried out by hand at a small scale to produce household commodities.

Laser-Based Additive Manufacturing: Modeling, Simulation, and Experiments, First Edition.
Narendra B. Dahotre, Mangesh V. Pantawane, and Shashank Sharma.

With the addition of machines, the scale of manufacturing surged dramatically during the first Industrial Revolution, which began in European countries in the eighteenth century and later spread to other parts of the world [Deane, and Deane, 1979]. This phase mainly centered around technologies that extracted metals (cast iron) from their natural forms (ores) and produced final products using industrial equipment. The improvement in the quality and characteristics of materials for the new types of applications and continuous production via conveyor equipment led to the second Industrial Revolution in the late nineteenth and early twentieth century [Popkova et al., 2019]. With the invention of techniques such as the Bessemer process to produce steel and electromagnetic rotary devices to electrify the technology, this phase was a technological revolution [Mokyr, 1998]. The second half of the twentieth century was driven mostly by renewable sources of energy and the emergence of digital technologies, constituting the third Industrial Revolution [Popkova et al., 2019]. The progress and features of the Industrial Revolutions are illustrated in Figure 1.1.

Today, in the early decades of the twenty-first century, AM is an integral part of the ongoing fourth Industrial Revolution. This new technological mode of manufacturing offers broad flexibility for materials science, process development, and structural design. Using AM, intricate and complex parts can be manufactured with the desired quality, which would be extremely challenging using earlier subtractive (machining) and formative (casting) manufacturing modes. Moreover, the inherent nature of AM is leading manufacturing toward fully automated digital manufacturing through robotic equipment. In contrast to earlier manufacturing techniques, which steadily evolved and advanced in response to challenges experienced by earlier versions, AM is an entirely new technique. Therefore, AM may be considered not an evolution but

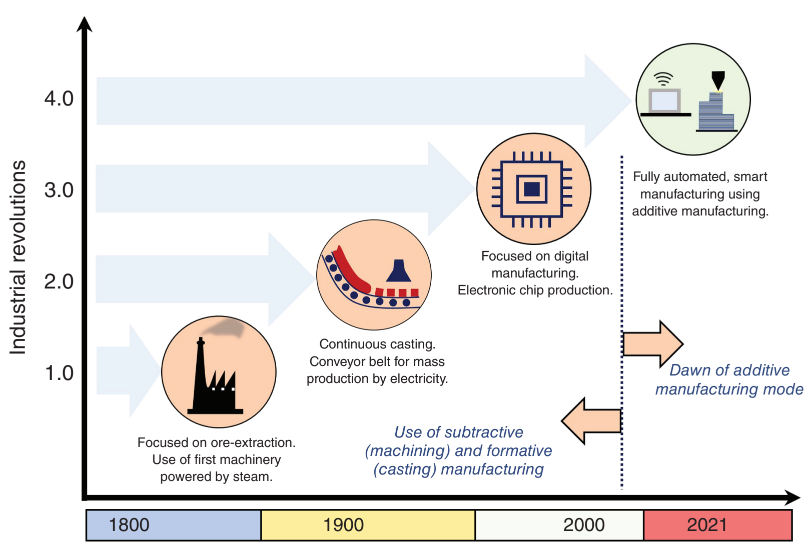

Figure 1.1 Timeline of the Industrial Revolutions.

the dawn of a new manufacturing era. Before diving deep into the technical features and current status of AM, we examine its intriguing fundamental nature in the following section.

1.2 Concept of AM

Although AM seems to be a new manufacturing mode in the twenty-first century, it existed silently as an auxiliary manufacturing technique for several decades in the previous century. The origin of all metallic AM types can be traced back and linked to welding and surface coating techniques. For instance, the friction stir AM technique evolved from friction stir welding and processing. These auxiliary manufacturing techniques were mature and only required a trigger to evolve into AM.

Eventually, AM was conceived as a fabrication method in the polymeric system in 1981 by Hideo Kodama, from Japan [Kodama, 1981]. He developed and demonstrated a prototype of the automatic fabrication of intricately shaped polymers, using layer-by-layer curing of the liquid and photo-hardening the polymer with ultraviolet rays. An intricate relief map of the mountain fabricated by Kodama using transparent polymer is presented in Figure 1.2. Charles Hull later advanced this technique and patented it as stereolithography (SLA) [Hull, 1984]. The concept of layer-upon-layer fabrication was then coupled with existing metallic welding and surface coating techniques, which led to the emergence of various metallic AM techniques.

The American Society for Testing and Materials (ASTM, an international standards organization primarily involved in developing and publishing voluntarily consensus technical standards for a broad range of materials, techniques, services, products, and systems), as per ISO/ASTM 52900:2015 (E), defines AM as “a process

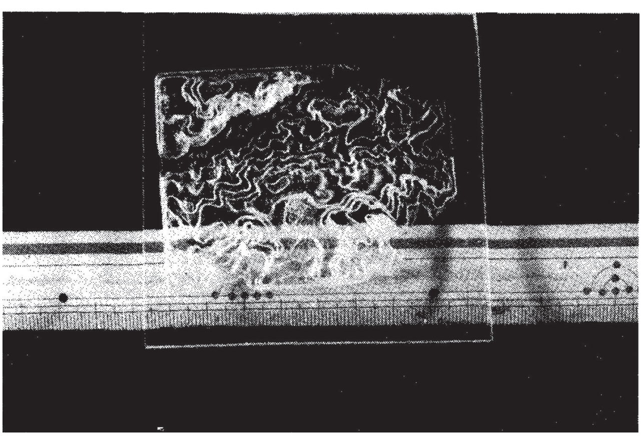

Figure 1.2 An early 3D fabrication via AM: a relief map of mountains using transparent polymer [Kodama, 1981].

of joining materials to make parts from 3D model data, usually layer upon layer, as opposed to subtractive manufacturing and formative manufacturing methodologies" [ASTM Standard, 2015]. Any material in its pure continuum/bulk form is held together by atomic bonds; for example, metal/alloys are bonded by metallic bonds, polymers by covalent and Van der Waal bonds, ceramics by ionic or covalent bonds, and composites by any combinations of these bonds. AM involves joining the material using a distinct physical phenomenon associated with an energy source that leads to the formation of such primary atomic bonds. The energy source can be in any of multiple forms (laser beam, electron beam, ultrasound, or friction); it is transformed into heat or a combination of heat and mechanical energy that joins the material through a primary atomic bond. This joining takes place at a micro- to macro-dimensional scale, depending on the type of energy source and the size and shape of pieces of unjoined material. These pieces of material in a feedstock[1] can be in forms such as powder (spherical particles), wires, rods, bars, and sheets. A moving interaction zone of energy and feedstock forms a single consolidated or joined track/line of material. The successive joining of such tracks in a single plane forms a fabricated layer of a given material. Eventually, this layer-upon-layer consolidation results in a three-dimensional component, and hence the name *additive manufacturing* was coined.

AM allows the flexibility of fabricating any intricate shape that can be created with the aid of CAD (computer-aided design) software. A virtual model of the part to be fabricated is converted into an STL[2] file format, which presents the geometry in a form the AM machines can understand to build the physical part. The STL file allows the AM machine to read the path of the interaction zone of energy and feedstock in a given layer as well as the dimensions and the number of layers to fabricate the geometry encrypted in the STL file. Given this path and the geometric dimensions, the machine allows the user to choose processing parameters such as power and the speed of the moving energy source. The feedstock provides additional flexibility depending on the material type, shape, and size distribution.

The various components of AM provide tremendous flexibility, and their combination can lead to multiple possible fabrication outcomes. These features of AM are as follows:

- Type of energy source
- Physical phenomenon
- Type of material (metal, ceramic, polymer, composite)
- Type of feedstock (shape, size, and distribution)
- Means of distributing the feedstock to interact with the energy source (already laid feedstock and simultaneous deposition of energy and feedstock)
- Combination of processing parameters (power of energy source, speed and path of energy-feedstock interaction zone, and feedstock input)
- Composition of material (alloy development)

1 A bulk of raw unjoined material that is consolidated/joined via AM to yield a final form.
2 This acronym is derived from STereroLithography. It is also sometimes defined as Standard Triangulation Language or Standard Tesselation Language.

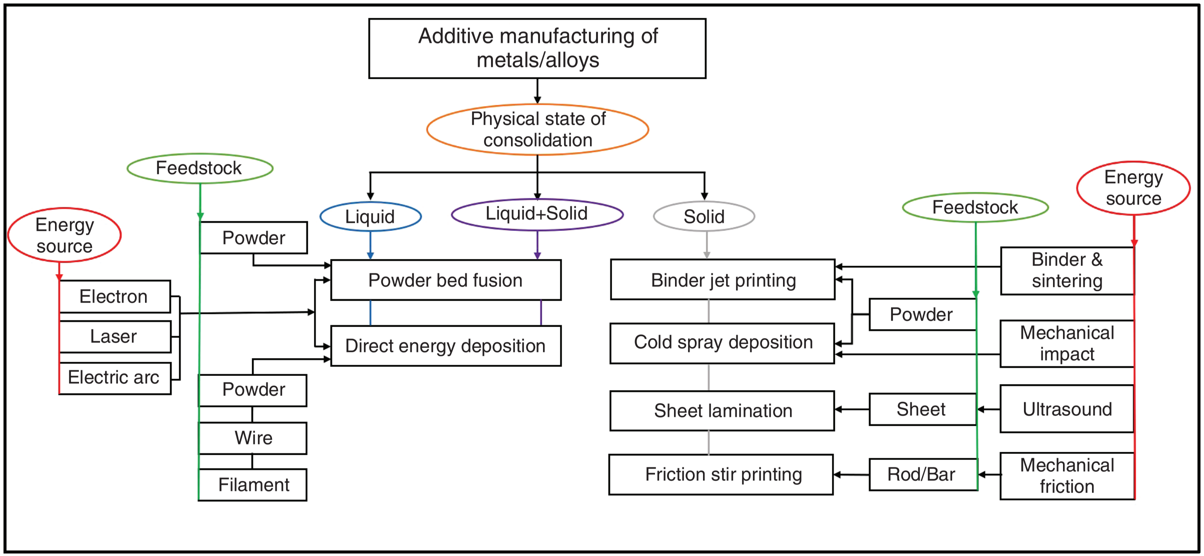

Figure 1.3 Classification of various AM techniques.

Categorization-These features also provide multiple bases for classifying different AM processes. As per ASTM/ISO standards, AM processes have the following seven categories:

- Binder jetting
- Directed energy deposition
- Material extrusion
- Material jetting
- Powder bed fusion
- Sheet lamination
- Vat polymerization

As mentioned earlier, the classification can have multiple forms based on various fundamental features. However, at this point, the reader should bear in mind the scope of the current book, which focuses on the AM of metals/alloys. There are multiple ways to classify the AM of metals and alloys, including classification based on the physical state of consolidation, energy source, feedstock, feedstock input, etc. Classification based on the physical phenomena governing the physical state of consolidation is useful from a materials science perspective. This is because the process-associated physical phenomena substantially control various properties of the AM-fabricated component. This classification based on the physical state of consolidation also considers the type of feedstock and the energy source, as shown in Figure 1.3.

1.3 Advantages over Conventional Manufacturing Techniques

Needless to say, the fundamental difference between AM and conventional manufacturing is due to their distinct processes and fabrication steps leading to the final component. Following are the key features that separate AM from conventional manufacturing.

- *Material efficiency*: The prime functional difference between these approaches arises from the substantially high material efficiency associated with the AM process, whereas conventional manufacturing results in more material loss through the subtractive approach in multiple steps.
- *Complex parts*: The layer-upon-layer approach of AM allows the fabrication of complex geometries, which are nearly impossible or highly challenging to fabricate using a conventional approach in a single processing step.
- *Assembly stage*: Traditionally, a moving system is required to manufacture in stages, first fabricating each component of the system and then assembling them. AM merges manufacturing and assembly into a single step, making a more efficient fabrication chain.
- *Customized printing*: AM provides the freedom to conceive any imaginable shape and make it a reality. In addition, customization through a digital interface allows

personalized products to be made for individuals. Conventional manufacturing does not provide such customization or the freedom to fabricate any shape.

- *Thermokinetic flexibility*: Most AM techniques provide process flexibility and, in turn, thermokinetic flexibility to derive the desired mechanical output from the process, whereas conventional techniques have limited options to vary the thermokinetics in a single step.

Presently, many AM techniques are available, and more are emerging. Among these AM techniques, laser-based AM (LAM) techniques are being widely explored, substantially impacting the research and industry sector. The laser is a rapidly steerable and effective energy source that provides high energy density in a micro-region. This allows microscale feedstock (powder and wire) to rapidly melt and solidify, leading to micro-volume consolidation of feedstock. Therefore, the type of energy source and feedstock used in LAM allow the rapid fabrication of complex geometry with the desired surface finish while providing increased efficiency in both cost and materials. LAM is also a single-step process that provides considerable flexibility through a broad processing window that can monitor the thermodynamic state, morphology, and distribution of the phases as well as the crystallographic and physical texture (surface roughness) of the printed component. The most commonly employed and investigated LAM techniques for fabricating metal/alloys are laser powder bed fusion (LPBF) and laser-based directed energy deposition (LDED). The fundamental principles and operation of these techniques are introduced in the following section.

1.4 Laser-Based AM

Recent advances in design and operation have led to numerous LAM techniques. They vary mostly based on the type, size, and delivery of the feedstock to the laser source. Despite these variations, a few physical phenomena associated with the process can be identified. Thus, LAM techniques can be classified as LPBF and LDED processes.

1.4.1 Laser-Based Directed Energy Deposition

LDED is also referred to as the direct metal deposition (DMD) technique, which evolved from the laser cladding technique in the late twentieth century [Koch, and Mazumder, 1993, Mazumder et al., 1997]. In LDED, the feedstock (usually a powder or wire) is delivered through a nozzle directly to the focal plane of the laser beam, as depicted in Figure 1.4. The powder is carried from the powder feeder via carrier gas, often coaxially focused at the focal region of the laser beam. As the name suggests, the purpose of the carrier gas, such as argon or nitrogen, is to carry the powder to its destination with sufficient momentum to hit the laser beam focal plane. Under the high power density of the laser beam at the focal plane, the powder instantly melts and falls onto the substrate, where it solidifies. This follows the fabrication of a layer through metal deposition via multiple laser tracks, and successive layer-upon-layer

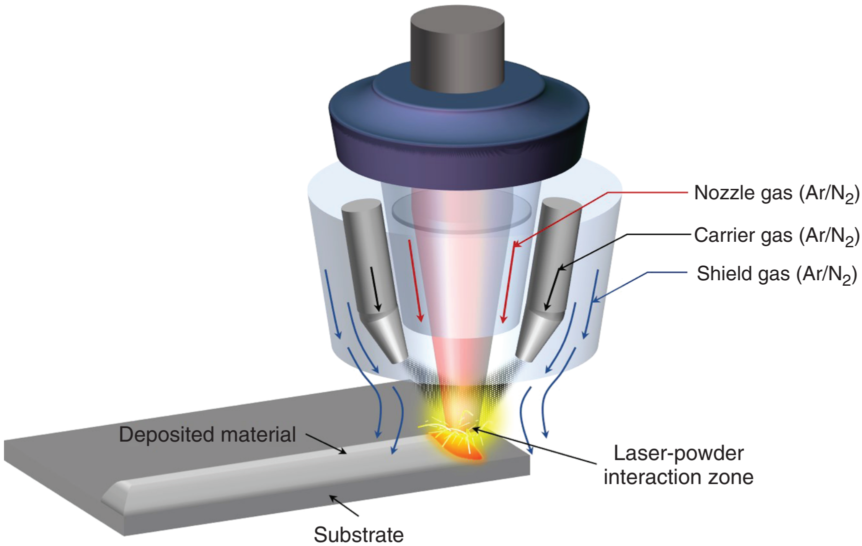

Figure 1.4 Schematic representation of the LDED operation using powder feedstock.

fabrication allows the formation of a 3D component. In most LDED machines, the substrate attached to the stage has three-axis (X, Y, and Z) freedom, while the laser head with the coaxial powder feeder remains stationary. The relative motion between the laser heat source and the stage leads to multiple laser tracks, and the layer thickness in the build direction is monitored by the STL file fed to the LDED machine.

The STL file allows the AM machine to monitor the three-axis stage movement with respect to the laser head. Nozzle gas (Ar/N_2) is often supplied to prevent damage to the laser optics caused by spatter ejected in the feedstock-laser interaction zone at the focal plane region. In addition, shield gas (Ar/N_2) prevents the feedstock-laser interaction zone and melt pool[3] region from oxidation. For most non-reacting (not easily oxidized) metals/alloys, shield gas is sufficient to prevent oxidation. However, such an assembly may not be able to prevent the oxidation of metals that have a high affinity for oxygen, such as Ti and Al. The fabrication of these alloys is often carried out in a closed chamber where oxygen activity can be set to as low as 50 ppm to reduce oxidation. Laser engineered net shaping (LENS) machines by Optomec provide a sealed assembly to fabricate oxidation-prone alloys via LDED.

The type of feedstock (powder or wire) can be varied in size depending on the delivery system to the laser beam source and laser characteristics such as wavelength, intensity distribution, beam diameter, etc. Such variations in the laser beam and feedstock (size and type) can lead to different dynamics, while the physical phenomena remain the same. Before the ASTM/ISO categorization

3 The melt pool is the melted region that results from heating by any heat source, surrounded by the solid material.

of this technique as a directed energy deposition, several names were introduced by researchers and companies trying to develop closed-loop machines. These names included LENS [Atwood et al., 1998], laser metal forming (LMF) [Gäumann et al., 2001], laser consolidation (LC) [Xue et al., 2000], laser direct casting (LDC) [Hand et al., 2000], automated laser powder deposition (ALPD) [Toyserkani, and Khajepour, 2006], shape deposition manufacturing (SDM) [Fessler et al., 1996], and so on. Although these processes had different names, their underlying principle was the same.

1.4.1.1 Machine Design

Modern evolving LDED machines have multiple degrees of freedom with the development of machine design; for instance, a five-axis stage system attached to the substrate. In contrast to the stationary (three-axis) stage, the five-axis system allows rotation of the stage; thus, support structures[4] are not required during fabrication [Liu et al., 2017]. In addition to stage rotation, the moving laser further augments the degree of freedom during fabrication, thereby allowing control over physical texture (surface roughness) and complexity of the component. In the LDED machine, the feedstock can be fed through either a coaxial nozzle or an off-axis lateral nozzle focusing at the laser beam focal plane. A powder-fed LDED machine can have single or multiple nozzles to eject the powder at the focal plane of the laser beam [Mazzucato et al., 2017]. Multiple nozzles with the appropriate use of inert gas lead to improved deposition efficiency by reducing the amount of unmelted powder, as it does not enter the laser-powder interaction zone and falls in the vicinity of the fabricating component. Moreover, multiple nozzles can eject different metal powders at different rates, allowing the fabrication of functionally graded components [Mahamood, and Akinlabi, 2015]. Furthermore, the substrate in LDED can be preheated to change the thermokinetics, especially the thermal gradients associated with the process [Corbin et al., 2018].

1.4.1.2 Process Parameters

Laser. In LDED, the laser is the source of energy used for the consolidation/joining (melting followed by solidification) of the feedstock. Different types of lasers can be employed in LDED fabrication, including Nd:YAG, CO_2, excimer, and fiber lasers. A Yb-doped fiber laser is most commonly employed after solid-state Nd:YAG laser in laser-based AM. Yb-fiber laser, usually pumped by the diodes in a 950-980 nm wavelength, can have an output wavelength in the near-infrared region ranging from 1030 to 1090 nm in a continuous wave or pulse wave mode. Every metal and alloy has a distinct light absorption coefficient at a given wavelength of light, determining the actual laser energy absorbed for melting. In LDED, laser parameters such as the laser power, laser beam diameter, laser intensity distribution (Gaussian or top-hat distribution), speed at which the laser beam moves relative to the substrate, and moving path can be easily varied and optimized to achieve the desired set of characteristics

4 Support structures are often incorporated in the STL file. However, they are not part of the actual 3D component. Support structures are often printed to the main component during fabrication to prevent part deformation and to ensure that it is attached to the substrate.

of a given material to be fabricated. The diameter of laser beam in LDED is often in the range of 0.5 to 5 mm, while the laser/stage moving speed varies from 5 to 20 mm/s. The laser power employed in LDED is usually high, in the range of 300 to 4000 W. Such a combination of process parameters yields a very high deposition rate in LDED.

Feedstock. Powder is most often used as a feedstock in LDED machines as it can fabricate small complex parts with high geometrical accuracy due to its micron-level size (40 to 120 μm). Such micron-sized powder allows the fabrication of thinner parts and simultaneously improves surface roughness. In addition, as discussed earlier, functionally graded material can be explored by feeding powder through multiple nozzles. However, this feedstock has several downsides, such as the high cost of powder preparation, health hazards, and significant loss of material during fabrication.

On the other hand, wire as a feedstock provides highly efficient material fabrication. Moreover, the production of wire feedstock is a simple, cleaner, cheaper process, and handling the wire is not hazardous. The wire is fed through the coaxial nozzle or the off-axis lateral nozzle, focusing at the laser beam focal plane. The diameter of the wire used for LDED feedstock ranges from 1 to 1.5 mm, which restricts the fabrication of thinner components, and the surface roughness is comparatively higher than powder-fed LDED [Rodrigues et al., 2020, Fu et al., 2021, Froend et al., 2018]. In contrast to powder feedstock, wire-fed LDED can be explored for underwater fabrication [Fu et al., 2021]. Nevertheless, wire-fed LDED is widely studied for its unique processing features.

The machine design features and process parameters associated with LDED provide tremendous flexibility to govern the thermokinetics, thermomechanics, and fluid dynamics of the process. These process-inherent physical phenomena affect microstructures; phase transformation; one- and two-dimensional crystallographic defects such as dislocations, twins, and stacking faults; grain/phase interfaces; and three-dimensional defects, including cracks and pores. These aspects, in turn, impact the mechanical and surface properties of the material. Thus, it is essential to know the degree of flexibility provided by the given LAM machine design and process parameters. These machine design and process parameters are detailed in Figure 1.5. The following chapters discuss the effect of machine design and process parameters on the microstructural characteristics listed previously with the aid of computational simulations.

1.4.2 Laser Powder Bed Fusion

LPBF is a widely studied LAM technique. As the name suggests, the feedstock in LPBF is limited to powder, mostly in the range of 10 to 45 μm. Unlike in the LDED technique, the feedstock (powder) is first spread onto the substrate as a thin layer that ranges from 10 to 100 μm. The laser selectively scans this layer. At the location scanned by the laser, the powder instantly melts and solidifies, thereby consolidating the scanned region. The substrate moves down within a hollow cylinder to occupy the powder for subsequent layer deposition. The unmelted powder surrounding the fused region provides support for the subsequent layer. When another layer is spread

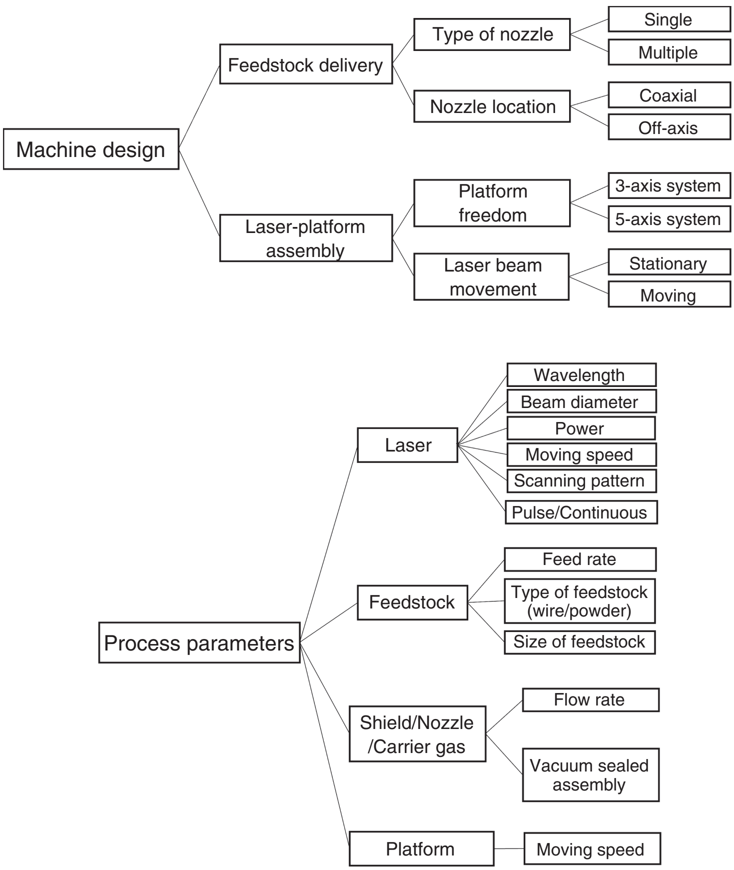

Figure 1.5 Machine design and process parameters associated with LAM.

onto a previously fused layer, the new layer is again scanned by the laser. The process continues until the desired component is built. The LPBF process is illustrated in Figure 1.6.

1.4.2.1 Process Parameters

The laser beam diameter in LPBF can vary from 30 to 600 μm, while the laser scanning speed can be as high as 200 to 4000 mm/s. The laser power varies in a range of 100 to 500 W. The resulting volume of the melt pool generated during LPBF is usually smaller than that of LDED. Therefore, the deposition rate in LPBF is often lower than that of LDED. However, LPBF produces a superior surface finish for the printed component than LDED. The smaller volume of the melt pool produced in LPBF also allows the fabrication of components with greater intricacy at the micron level. All of these process parameter differences in LDED and LPBF are summarized in Table 1.1.

The machine and process design in LPBF do not allow the powder stage to have any axis of freedom, unlike the three-axis and five-axis freedom in the LDED process.

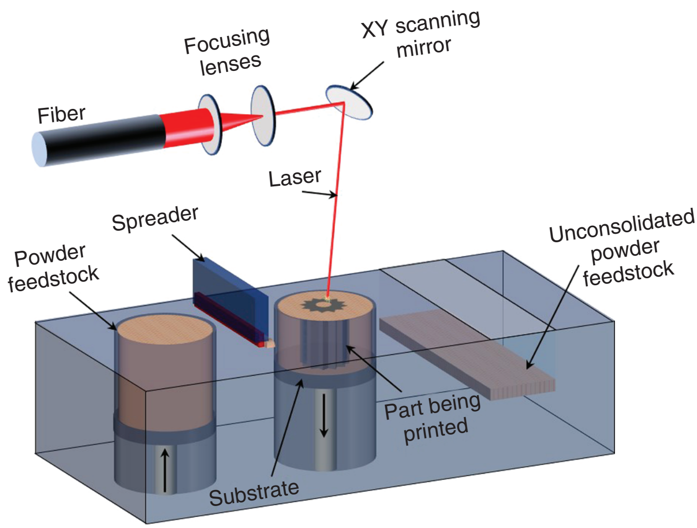

Figure 1.6 Schematic representation of a laser powder bed fusion process.

Table 1.1 Comparison of the processing parameters involved in the LDED and LPBF processes.

Parameters	**LDED**	**LPBF**
Laser power (W)	300–4000	100–500
Scanning speed (mm/s)	5–20	200–4000
Laser beam diameter (μm)	500–5000	30–600
Deposition rate	High	low
Surface finish	Moderate	Superior
Feedstock	Wire, powder	powder
Powder size (μm)	45–120	10–45

Source: [Bian et al., 2017]

The stage freedom in LDED allows variable thermokinetics in different directions. Nevertheless, a similar effect can be achieved in LPBF by varying the orientation of the component to be printed with respect to the build direction. For instance, a cylindrical component can be printed in different orientations with respect to the constant build direction, as illustrated in Figure 1.7. The printing component can be oriented to allow heat extraction in the desired direction, which, in turn, governs the crystallographic texture within the component.

Additionally, the powder bed stage in LPBF can be heated to any temperature at the beginning or any time during fabrication, allowing superior control over the thermokinetics of the process. The powder bed is often heated to reduce the thermal gradient, thereby reducing induced thermal stresses to avoid the formation of thermal cracks. Heating during the powder bed stage provides

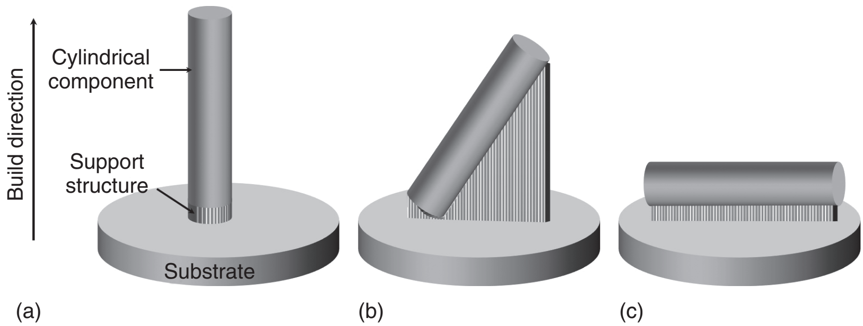

Figure 1.7 Different ways of printing a cylindrical component via laser powder bed fusion.

tremendous thermokinetic control, which, in turn, influences the thermodynamic state (equilibrium/non-equilibrium) of the phases formed during the process.

1.4.3 Estimation of Energy Input in LAM Processes

When optimizing fabricated parts for various properties, recognizing the energy input of the given LAM process is important. Energy input must consider the laser processing parameters to yield the energy density needed to fabricate the material. In the LDED process, the laser energy input is presented in multiple forms. One of them is the power density, also known as irradiance (W/m^2), which can be obtained as

$$Power\ Density\ or\ Irradiance = \frac{P}{A} \tag{1.1}$$

where P is the laser power (W) and A is the cross sectional area (m^2) of the laser beam exposed to the material.

Residence time (t_r) is another helpful parameter considered in multiple energy input representations. It is simply the duration for which a laser beam is exposed to a single location while scanning the sample. This can be calculated using the laser beam diameter (D) and laser scanning velocity (V_s):

$$t_r = \frac{D}{V_s} \tag{1.2}$$

Another way to represent energy input is laser fluence (F), which is energy density. Laser energy fluence can also be defined as a time-integrated energy flux. Therefore, the residence time is helpful to obtain the energy density/laser fluence:

$$F = \frac{P \times t_r}{A} \tag{1.3}$$

In addition, linear energy density (LED) (in J/m) is also considered as a parameter during property optimization and can be obtained as

$$LED = \frac{P}{V_s} \tag{1.4}$$

For the LPBF process, while the previous energy input parameters are appropriate, most researchers use volumetric energy density as the energy input parameter, considering the layer thickness (d) and hatch spacing (h). This volumetric energy density (VED) is calculated as follows:

$$VED = \frac{P}{V_s \times h \times d} \tag{1.5}$$

However, the energy parameter *VED* bears some limitations, as identified by several studies [Scipioni Bertoli et al., 2017, Caiazzo et al., 2020, Prashanth et al., 2017, Ferro et al., 2020]. Some of these studies have recognized another way to represent VED by following Eq. 1.6:

$$VED = \frac{P}{V_s \times h \times D} \tag{1.6}$$

While several energy parameter representations exist, none can represent the kinetics and physics associated with the process. Each of these parameters is significant in optimizing and designing various features of the components and their characteristics.

LAM processes assisted by the pulse wave (PW) laser beam entail additional parameters as their energy transfer mechanism differs from that of a continuous-wave laser beam. A pulse laser provides considerable flexibility with its additional parameters. These parameters can be conveniently understood through the energy transfer mechanism of the pulse laser shown in Figure 1.8. In contrast to a continuous-wave laser, which delivers constant power P as indicated by the dotted red line, the pulse laser transfers energy in controllable intervals (Figure 1.8). This involves the pulse on time (t_{on}) when it delivers the power and the pulse off time (t_{off}) when power = 0. Thus, the pulse energy E_{pulse} is given as

$$E_{pulse} = \int_0^{t_{on}} P(t)dt \tag{1.7}$$

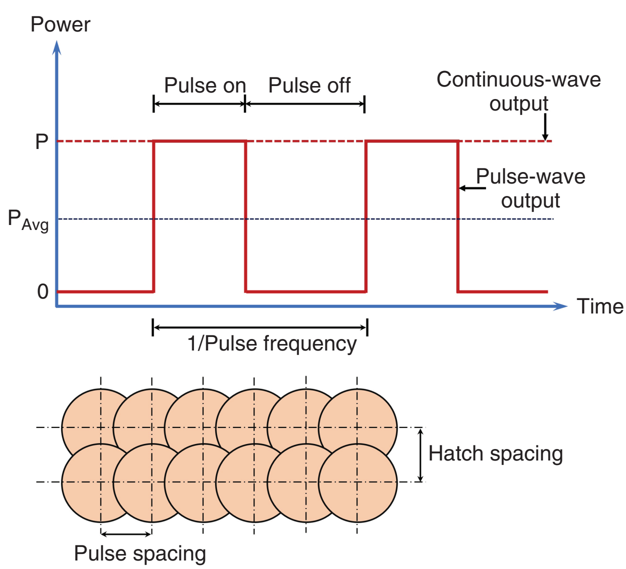

Figure 1.8 schematic of the temporal and spatial characteristics of pulses.

The pulse frequency or pulse repetition rate is the parameter that is often used during pulsing operation and is expressed as

$$\textit{Pulse Frequency} = \frac{1}{t_{on} + t_{off}} \tag{1.8}$$

The duty cycle (δ_d) is another important parameter employed during the PW-LAM process. It is presented as

$$\delta_d = \frac{t_{on}}{t_{on} + t_{off}} \tag{1.9}$$

With pulse frequency, one can obtain the average power delivered by the pulse laser (indicated by a black dotted line in Figure 1.8) as

$$P_{avg} = E_{pulse} \times \textit{Pulse Frequency} \tag{1.10}$$

In pulse laser operation, a single laser track exposure consists of multiple overlapped pulses. Thus, pulse overlapping occurs based on the pulse spacing, i.e. the distance between the centers of two consecutive pulses. The distance between the centers of tracks of pulses is the hatch spacing (h), shown in Figure 1.8. All of these parameters, such as power, pulse frequency, duty cycle, and pulse spacing, are unique to pulse laser operation and can be varied. During pulse laser operation, the scanning speed becomes irrelevant in terms of its direct correlation with any solidification parameter. In contrast, the same parameter is of significant interest when operated in continuous-wave mode as it is directly related to the solidification rate. Nevertheless, the average scanning speed in pulse laser operation can be obtained as

$$V_{avg} = \frac{\textit{Pulse Spacing}}{t_{on} + t_{off}} \tag{1.11}$$

1.4.4 Multi-Step LAM Techniques

The LAM techniques (LDED and LPBF) are often regarded as single-step processes because they involve manufacturing in a single operation considering the intended shape and size of the product [ASTM Standard, 2015]. Some LAM techniques involve multi-step processes, as fabricating the final product may require two or more steps. These multi-step LAM techniques involve forming the green (unconsolidated) shape of the product followed by consolidation through any physical phenomena to form the metallurgical bond.

Selective laser sintering (SLS), a multi-step LAM technique, works on the same principle mentioned earlier [Bian et al., 2017]. The formation of the green component in SLS can involve liquid phase sintering or partial melting. The former uses a mixture of sacrificial polymeric binder (in powder form) and metal powder particles. Upon laser exposure, the binder melts and spreads over the powdered metal particles and holds them with a secondary bond as it solidifies while cooling. As the metal particles do not melt, sintering of the particles occurs while the solidified binder holds them with the secondary bond. On the other hand, during partial melting, the powdered metal particles are partially melted, and their surfaces are fused upon solidification. The green part fabricated via both the processes has 50% or greater porosity. The green part formed by the binder undergoes heating and isothermal heat treatment at a temperature high enough to vaporize the binder, known as the debinding process, to create the brown part. This follows further heat treatment of the part to increase the densification by sintering. Debinding is not required for a green part processed via partial melting of particles by laser. However, the SLS process cannot produce a fully dense part, as the density is limited to 80%. Additional steps in the SLS process, such as hot isostatic pressing (HIP), can further increase the density of the part [Bian et al., 2017].

Based on the description of the SLS and SLS/HIP processes, it is apparent that they do not provide thermokinetic flexibility via processing, which is the prime feature of LDED and LPBF. Moreover, due to its cost, the SLS technique does not fit in among other, cost-efficient rapid prototyping techniques. In addition to being porous and brittle, SLS-fabricated components are often left with thermal distortion, warping, and shrinkage. Consequently, obtaining a near-net-shape is a challenge. The capital cost associated with the machine and its maintenance makes the process expensive and inefficient. Despite the multiple disadvantages, SLS has been gradually improving due to recent innovation and development. However, it is still noteworthy that the SLS process inherently does not allow the thermokinetic flexibility to achieve the desired microstructure. SLS thermokinetics are more relatable to those achieved during traditional isothermal heat treatment.

With the brief introduction to AM and LAM presented in this chapter, one can recognize the true potential of AM over the existing conventional manufacturing techniques. The versatility of the LAM technique through machine design, process parameters, and feedstocks allows the accurate fabrication of any conceivable geometry. Although understanding of LAM techniques viewed through the lens of material science is increasing, these techniques are still in their infancy. Computational material science has played a pivotal role in further expediting this understanding. Hence, Chapter 2 of this book is dedicated to a detailed understanding of computational material science.

References

ASTM Standard. (2015). Standard terminology for additive manufacturing-general principles-terminology. ASTM F42 Committee, ASTM International.

Atwood, C., Griffith, M., Harwell, L. et al. (1998). Laser engineered net shaping (LENS™): A tool for direct fabrication of metal parts. In: *International Congress on Applications of Lasers & Electro-Optics*, E1–E7. Laser Institute of America.

Bian, L., Shamsaei, N., and Usher, J. (2017). *Laser-Based Additive Manufacturing of Metal Parts: Modeling, Optimization, and Control of Mechanical Properties*. CRC Press.

Caiazzo, F., Alfieri, V., and Casalino, G. (2020). On the relevance of volumetric energy density in the investigation of Inconel 718 laser powder bed fusion. *Materials* 13 (3). https://www.ncbi.nlm.nih.gov/pmc/articles/PMC7040579/.

Corbin, D.J., Nassar, A.R., Reutzel, E.W. et al. (2018). Effect of substrate thickness and preheating on the distortion of laser deposited Ti–6Al–4V. *Journal of Manufacturing Science and Engineering* 140 (6).

De la Torre, I. (2011). The origins of stone tool technology in africa: a historical perspective. *Philosophical Transactions of the Royal Society B: Biological Sciences* 366 (1567): 1028–1037.

Deane, P.M. and Deane, P.M. (1979). *The First Industrial Revolution*. Cambridge University Press.

Ferro, P., Meneghello, R., Savio, G. et al. (2020). A modified volumetric energy density-based approach for porosity assessment in additive manufacturing process design. *International Journal of Advanced Manufacturing Technology* 110 (7–8): 1911–1921. https://doi.org/10.1007/s00170-020-05949-9.

Fessler, J., Merz, R., Nickel, A. et al. (1996). Laser deposition of metals for shape deposition manufacturing. In: 1996 *International Solid Freeform Fabrication Symposium*, 117–124. University of Texas at Austin.

Froend, M., Riekehr, S., Kashaev, N. et al. (2018). Process development for wire-based laser metal deposition of 5087 aluminium alloy by using fibre laser. *Journal of Manufacturing Processes* 34: 721–732.

Fu, Y., Guo, N., Wang, G. et al. (2021). Underwater additive manufacturing of Ti-6Al-4V alloy by laser metal deposition: Formability, grain growth and microstructure evolution. *Materials & Design* 197: 109196.

Gäumann, M., Bezencon, C., Canalis, P., and Kurz, W. (2001). Single-crystal laser deposition of superalloys: processing–microstructure maps. *Acta materialia* 49 (6): 1051–1062.

Hand, D., Fox, M., Haran, F. et al. (2000). Optical focus control system for laser welding and direct casting. *Optics and lasers in Engineering* 34 (4–6): 415–427.

Hull, C.W. (1984). Apparatus for production of three-dimensional objects by stereolithography. United States Patent appl. 638905.

Koch, J. and Mazumder, J. (1993). Rapid prototyping by laser cladding. In: *International Congress on Applications of Lasers & Electro-Optics*, 556–565. Laser Institute of America.

Kodama, H. (1981). Automatic method for fabricating a three-dimensional plastic model with photo-hardening polymer. *Review of Scientific Instruments* 52 (11): 1770–1773.

Liu, R., Wang, Z., Sparks, T. et al. (2017). Aerospace applications of laser additive manufacturing. In: *Laser Additive Manufacturing*, 351–371. Elsevier.

Mahamood, R. and Akinlabi, E.T. (2015). Laser metal deposition of functionally graded Ti6Al4V/TiC. *Materials & Design* 84: 402–410.

Mazumder, J., Choi, J., Nagarathnam, K. et al. (1997). The direct metal deposition of H13 tool steel for 3-D components. *JOM* 49 (5): 55–60.

Mazzucato, F., Marchetti, A., and Valente, A. (2017). Analysis of the influence of shielding and carrier gases on the ded powder deposition efficiency for a new deposition nozzle design solution. In: *International Conference on Additive Manufacturing in Products and Applications*, 59–69. Springer.

Mokyr, J. (1998). The second industrial revolution, 1870–1914. In: *The Lever of Riches: Technological Creativity and Economic Progress*, 1–18. Oxford University Press.

Popkova, E.G., Ragulina, Y.V., and Bogoviz, A.V. (2019). Fundamental differences of transition to industry 4.0 from previous industrial revolutions. In: *Industry 4.0: Industrial Revolution of the 21st Century*, 21–29. Springer.

Prashanth, K.G., Scudino, S., Maity, T. et al. (2017). Is the energy density a reliable parameter for materials synthesis by selective laser melting?. *Materials Research Letters* 5 (6): 386–390. https://www.tandfonline.com/action/journalInformation?journalCode=tmrl20.

Rodrigues, M.B., Silva, R.G.N., Pereira, M. et al. (2020). Effect of dynamic wire feeding on deposition quality in laser cladding process. *Journal of Laser Applications* 32 (2): 022065.

Scipioni Bertoli, U., Wolfer, A.J., Matthews, M.J. et al. (2017). On the limitations of volumetric energy density as a design parameter for selective laser melting. *Materials and Design* 113: 331–340.

Toyserkani, E. and Khajepour, A. (2006). A mechatronics approach to laser powder deposition process. *Mechatronics* 16 (10): 631–641.

Xue, L., Chen, J., Islam, M. et al. (2000). Laser consolidation of in-738 alloy for repairing cast IN-738 gas turbine blades. In: *Proceedings of 20th ASM Heat Treating Society Conference, St.-Louis, Missouri, USA*, 1063–1071. ASM.